The Egyptian Journal of Hospital Medicine (October 2025) Vol. 101, Page 5265-5275

Role of Susceptibility Weighted Imaging in Evaluation of Patients with Multiple Sclerosis

Hayam A. Abdellatif, Zeinab A. Aly, Sarah R. Sendersy
Interventional Radiology and Medical Imaging, Faculty of Medicine, Menoufia University, Menoufia, Egypt
***Corresponding author:** Sarah Sendersy, **Tel:** +20 1025383033, **E-mail:** sarasendersy@gmail.com

ABSTRACT

Background: Multiple Sclerosis (MS) is an inflammatory autoimmune disease involving multifocal demyelination and neuronal loss. Routine MRI detects lesions, yet newer modalities like Susceptibility-Weighted Imaging (SWI) offer insight into vascular and iron pathology.

Aim: This study aimed to determine the utility of SWI in the detection of signs of CVS and PRL in patients with MS, and its comparison with 3D FLAIR for lesion detection.

Methods: A prospective study included 50 clinically confirmed MS patients (age 11–52 years) who underwent standard MRI, supplementary 3D FLAIR, and SWI. Fifteen participants also received contrast-enhanced T1 imaging. Lesions were evaluated for total count, CVS, and paramagnetic rim lesion (PRL) presence. Sensitivity and lesion characteristics of 3D FLAIR and SWI were contrasted, and correlations with patient age and lesion burden were computed

Results: 3D FLAIR detected a slightly larger total number of lesions (1,084 vs. 1,050) and median number of lesions per patient (25 vs. 20; $p = 0.004$). SWI demonstrated superior detection of CVS-positive lesions (median 9.5 vs. 3.5; $p < 0.001$), with CVS in 90% and PRLs in 74% of subjects. SWI alone detected iron-related pathology and vascular involvement, contributing to lesion count provided by 3D FLAIR.

Conclusion: SWI augments conventional MRI in MS evaluation with added specificity through CVS and paramagnetic rim depiction, echoing vascular and chronic inflammation activity. Synthesis of 3D FLAIR for lesion load and SWI for iron- and vein-related observations optimizes diagnosis and prediction assessment, making routine incorporation of SWI in MS imaging protocols a preferred option.

Keywords: Multiple sclerosis, Susceptibility-weighted imaging, SWI, 3D FLAIR, Central vein Sign, Paramagnetic rim lesions.

INTRODUCTION

Multiple Sclerosis (MS) is the most prevalent inflammatory, autoimmune neurological disorder that primarily affects young and middle-aged adults, although it can also manifest in older individuals. Pathologically, MS is defined by multifocal inflammation, demyelination, axonal injury and subsequent neuronal loss. The diagnosis requires objective evidence demonstrating that the lesions are disseminated both in time and in space. Conventional Magnetic Resonance Imaging (MRI) is highly sensitive for demonstrating this dissemination of lesions over time and space [(1)].

MS exhibits a characteristic distribution of white matter lesions which is useful for differentiating them from vascular lesions. MS typically involves the corpus callosum, U-fibers (juxtacortical), temporal lobes, brainstem, cerebellum, and spinal cord. This pattern of involvement is unusual in other diseases. In the case of small vessel disease, while the brainstem may be affected, the involvement is usually symmetrical and central, whereas in MS, the lesions tend to be peripheral [(2)].

Conventional MRI methodologies maintain a pivotal function in both the initial diagnosis and the subsequent longitudinal monitoring of disease progression and evolution in MS [(3)]. A thorough and systematic analysis of the specific morphological and signal characteristics of MS lesions observed on these standard images offers a valuable non-invasive insight into the complex spectrum of underlying acute and chronic neuropathology. The presence of hyperintense lesions identified on T2-weighted images (T2w) constitutes a hallmark radiological feature utilized for the diagnosis of MS. However, these hyperintensities are understood to represent a complex and heterogeneous mixture of underlying tissue pathology. This spectrum of changes encompasses acute processes, such as vasogenic edema, alongside chronic and irreversible alterations, including reactive gliosis, significant axonal loss and the defining pathology of demyelination [(4)]. New T2 lesions on follow-up MRI are commonly employed in the search for recent inflammatory disease activity. In addition, the presence of contrast enhancement on post-contrast T1-weighted (T1w) images and occasionally hyperintensity on diffusion-weighted MRI can also indicate acute inflammatory changes [(5)].

The advanced neuroimaging technique of Susceptibility-Weighted Imaging (SWI) has recently demonstrated a heightened sensitivity to the accumulation of magnetic substances, particularly various forms of iron, including ferritin, hemosiderin, and deoxyhemoglobin [(6)]. This methodological capacity enables the detection of iron deposits across multiple compartments within the central nervous system affected by MS. Specifically, iron accumulation has been observed within the demyelinating lesions, the surrounding normal-appearing brain tissue (NABT) and notably concentrated

Received: 23/05/2025
Accepted: 25/07/2025

in the vessel walls of cerebral veins. The underlying mechanism posited for iron-mediated damage is the catalysis of highly reactive free radicals through Fenton chemistry. This process consequently induces severe oxidative stress, which is directly toxic to oligodendrocytes and results in the subsequent destruction of the protective myelin sheath [(7)]. The ability to visualize these iron-rich regions offers a powerful, non-invasive means for monitoring localized oxidative injury and disease progression. Furthermore, areas of active myelin breakdown also show susceptibility effects in the form of dark dots or rims. The susceptibility effects in those lesions are due to the presence of iron-laden activated macrophages and reactive astrocytes at the lesion edge [(8)].

SWI offers supplementary information beyond the standard contrasts provided by conventional MRI. This advanced imaging technique can identify central veins within lesions, and recent evidence suggests that MS lesions may be identifiable by a phase rim surrounding the lesion [(9)]. When utilized following the application of a contrast agent, SWI provides additional insights into MS pathology. The visualization of veins connected to lesions is a potentially useful marker in the differential diagnosis of MS, being observed in approximately half of the enhancing lesions [(10)].

Susceptibility artifacts, which appear as hypointense dots both within and at the periphery of the lesion, are hypothesized to indicate the presence of myelin-laden macrophages and ongoing smoldering inflammation. Therefore, SWI has the potential to provide clinically relevant additional information for evaluating the status of lesions in MS patients [(11)]. Thus, the aim of this study was to evaluate the role of susceptibility-weighted magnetic resonance imaging (SWI) in the assessment of patients with MS.

PATIENTS AND METHODS

This prospective study was conducted on fifty clinically definite MS patients according to McDonald's criteria and clinical assessment, 34 women and 16 men aged between 11 and 52 years. All patients underwent clinical brain MRI scans, including T1W, T2W, FLAIR, and DWI, in the Radio-diagnosis Department, Faculty of Medicine, Alexandria University, as well as private radiology centers in Alexandria and Damanhur from January 2024 to December 2024. In addition to conventional MRI sequences, patients were also exposed to 3D FLAIR and SWI to achieve simultaneous phase and magnitude images. Fifteen patients underwent contrast-enhanced MRI scans and a post-contrast axial T1 sequence was also acquired.

The McDonald criteria for patients in terms of disease location and duration were the **inclusion criteria** [(12)]. By the 2017 McDonald criteria, dissemination in space is defined as having at least one hyperintense lesion on T2 or FLAIR of ≥ 3 mm in maximal diameter within two or more of the following CNS areas: Periventricular, cortical or juxta-cortical, infratentorial, or spinal cord. For individuals above the age of 50 years, increased numbers of lesions are advised. It is noteworthy that T2-hyperintense optic nerve lesions, such as those due to optic neuritis, could not be used to meet the 2017 modified McDonald criteria. Dissemination in time is confirmed either by a new T2-hyperintense or enhancing lesion compared to a baseline MRI or by the coexistence of both Gd-enhancing and non-enhancing T2-hyperintense lesions on a single MRI scan.

Exclusionary criteria: Indefinite MS cases that failed the radiological and clinical diagnosis, or any contraindication for MRI like cardiac implantable electronic devices, metallic intraocular foreign body, cochlear or ear implants, or magnetic dental implants.

All patients underwent thorough clinical evaluation, including full history taking and thorough examination of visual impairment, general weakness, fatigue, weakness of muscles and paresthesias along with documentation of age, gender, and other epidemiologic data. The brain MRI was performed with a routine quadrature head coil, with the patient heads in a vacuum pillow to prevent mal-rotation. Imaging protocol was axial and coronal T2-weighted images (TR = 5458 ms, TE = 110 ms, slice thickness = 6 mm, FOV = 230 mm), axial and sagittal FLAIR (TR = 10000 ms, TE = 140 ms, TI = 2800 ms, slice thickness = 6 mm, FOV = 230 mm), sagittal and axial T1-weighted images (TR = 565 ms, TE = 12 ms, slice thickness = 6 mm, FOV = 230 mm) and DWI with ADC maps (TR = 8300 ms, TE = 90 ms, slice thickness = 5 mm, FOV = 221×260, B values 0, 500, 1000, 1500). Other series were axial SWI (TR = 52 ms, TE = 12 ms, slice thickness = 2.4 mm, FOV = 230 mm, scanning time 2 min 32 sec), 3D FLAIR (TR = 8000 ms, TE = 355 ms, refocusing angle 50°, spatial resolution 1×1×2 mm, reconstructed resolution 1×1×1 mm) and post-contrast T1-weighted images after intravenous administration of Gadobutrol (0.1 mmol/kg in 1 min, TR = 565 ms, TE = 12 ms, slice thickness = 6 mm, FOV = 230 mm) [(13)].

Image analysis was performed, SWI sequences were used to measure the number and ratio of visible central veins and intra-lesional iron within lesions, further divided into paramagnetic rims and core lesions [(14)]. Confluent lesions were counted if there were one central vein or one of its "fingers" visible, and those with diameter less than 3 mm in the shortest axis were excluded. Paramagnetic rims were described as hypointense ring-like signals that completely or partially surround lesions, whereas core lesions were observed as

central nodular hypo-intensities within the center of FLAIR hyperintense lesions and being thicker than central veins without a tubular morphology. All paramagnetic rim lesions were also assessed for activity by DWI to detect diffusion restriction and post-contrast T1 images to detect enhancement if possible. The appearance of central veins on 3D FLAIR and SWI were compared to determine the optimal sequence for the detection of central vein sign. Sensitivity measurements of both sequences were approximated using the 45% rule, 3-lesion rule, and 6-lesion rule, which are recommended in the diagnosis of MS. Age correlated with the number of lesions showing central veins and lesions with iron-containing lesions, and number of paramagnetic rims lesions correlated with total lesion burden.

Ethical approval: The research was approved by Menoufia University Faculty of Medicine Ethical Committee and the Institutional Review Board (IRB) of Menoufia Faculty of Medicine (Approval No.: 5/2024RADIO). This entire body of work was carried out in accordance with The Code of Ethics of the World Medical Association (Declaration of Helsinki). To ensure respect for patient autonomy, all participants were provided with comprehensive and clear explanations regarding the study's specific objectives, overarching aims, and detailed methodology. Subsequently, their voluntary written informed consents were obtained prior to their formal enrollment in the investigation.

Statistical analysis

Data were analyzed using SPSS version 25.0. Descriptive statistics were calculated for demographic variables, with results presented as means ± standard deviation (SD) for continuous data and frequencies with percentages for categorical data. The Wilcoxon signed-rank test, a non-parametric alternative to the paired t-test was employed to compare paired data from 3D FLAIR and SWI MRI sequences including lesion counts and central vein sign (CVS) detection per patient due to the non-normal distribution of the data. Spearman's rank correlation coefficient was used to assess relationships between age and both the proportion of CVS-positive lesions and the number of paramagnetic rim-positive lesions. $P \leq 0.05$ was deemed significant.

RESULTS

This study included 50 with clinically definite MS patients based on the McDonald criteria. Table (1) presented the demographic characteristics of the examined 50 patients. The majority were female (68.0%), indicating a potential sex-related prevalence or selection bias in the studied population. The age range was broad (11–52 years), with a mean age of 37.34 ± 9.56 years, suggesting that the condition under investigation affects a wide age spectrum, primarily middle-aged individuals.

Table (1): Distribution of the studied cases according to demographic data in the examined (50) patients

Demographic data	
Sex	
Male	16(32.0%)
Female	34 (68.0%)
Age (years)	
Minimum – Maximum	11 – 52
Mean ± SD	37.34 ± 9.56

Table (2) and figure (1) presented a comparison of lesion visibility between 3D FLAIR and SWI MRI sequences across 50 patients. While the total number of lesions identified was slightly higher with 3D FLAIR (1,084 vs. 1,050), both sequences failed to detect lesions in the same two patients, indicating similar sensitivity for lesion presence. However, the median number of lesions per patient was significantly higher on 3D FLAIR (25) compared to SWI (20), with a statistically significant difference (p = .004). The range of lesion counts per patient was identical (0–55) in both modalities, suggesting that while both methods detected a similar spread of lesion burden, 3D FLAIR demonstrated superior lesion conspicuity or detectability on a per-patient basis.

Table (2): Comparison of lesion visibility on 3D FLAIR vs. SWI

	3D FLAIR	**SWI**	**P-Value (Wilcoxon)**
Total Lesions Identified	1,084 lesions	1,050 lesions	
Patients with No Visible Lesions	2 patients	2 patients	
Median Lesions per Patient	25	20	0.004*
Lesion Count Range per Patient	0 – 55	0 - 55	

*statistically significant Wilcoxon Signed-Rank Test.

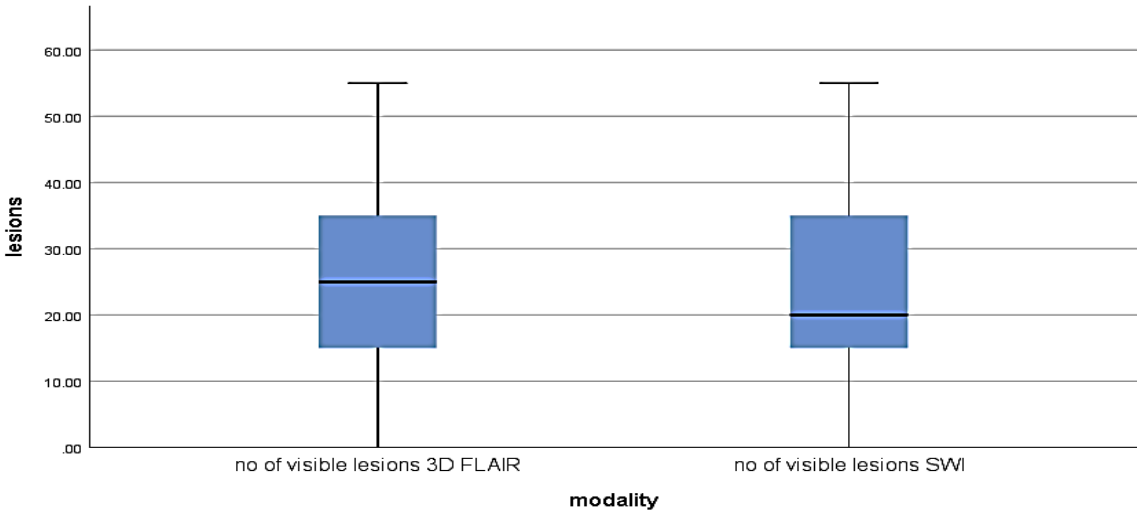

Figure (1): Box plot showing the comparative frequency (median and interquartile range) of the number of visible MS lesions between 3D FLAIR and SWI sequence.

Table (3) and figure (2) presented a comparison of Central Vein Sign (CVS) detection between 3D FLAIR and SWI sequences. The results demonstrated a markedly higher detection rate of CVS-positive lesions on SWI, with a mean percentage of 8.92% compared to 3.50% on 3D FLAIR. Similarly, the median number of CVS-positive lesions per patient was significantly higher on SWI (9.50) versus 3D FLAIR (3.50). The Wilcoxon signed-rank test indicated this difference was statistically significant (p = .000), confirming that SWI is more sensitive in detecting CVS. The range of detected lesions also extended further on SWI (0–20) than on 3D FLAIR (0–12), reinforcing the superiority of SWI in visualizing peri-venular lesions.

Table (3): Comparison of central vein sign (CVS) detection on 3D FLAIR vs. SWI sequences

Parameter	3D FLAIR	SWI	P-Value (Wilcoxon)
Mean % of Lesions Showing CVS	3.50	8.92	
Median No. of CVS-Positive Lesions/Patient	3.50	9.50	.000*
Range of CVS-Positive Lesions per Patient	0.00–12.00	0.00–20.00	

*statistically significant Wilcoxon Signed-Rank Test.

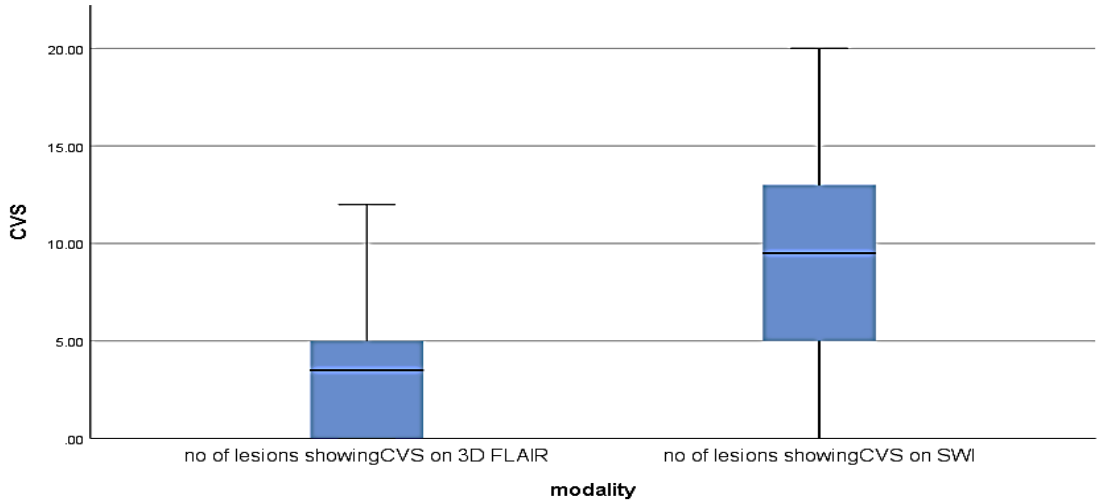

Figure (2): Box plot demonstrating the comparative frequency (median and interquartile range) of number of peri-venular lesions in MS patients using SWI and 3D FLAIR sequence. Points outside the boxplots represent the outliers within their groups

Table (4) presented a comparative analysis of lesion detection between 3D FLAIR and SWI MRI sequences, revealing that SWI was significantly more effective in identifying lesions with the central vein sign (CVS), a key marker in diagnosing multiple sclerosis (median 9.5 vs. 3.5, p = .000). In contrast, 3D FLAIR detects a higher overall number of visible lesions (median 25 vs. 20, p = .004), suggesting its strength in assessing total lesion burden. These findings underscored the complementary value of both sequences in neuroimaging: SWI for specificity and 3D FLAIR for sensitivity.

Table (4): Comparison of lesions parameters between 3D FLAIR and SWI sequences

Parameter	3D FLAIR	SWI	p-value
Number of Lesions Showing CVS			
Median	3.50	9.50	.000*
(Min-Max)	(0–12)	(0–20)	
Number of Visible Lesions			
Median	25	20	.004*
(Min-Max)	(0–55)	(0–55)	

The majority of patients (90.0%) demonstrated a positive central vein sign (CVS) on SWI, indicating a high prevalence of this imaging marker in the studied population. Additionally, a para-magnetic rim was observed in 74.0% of cases, further supporting its potential diagnostic value. The relatively lower frequency of rim presence compared to CVS may reflect differing sensitivities of these markers for underlying pathological processes (Table 5 & figure 3)).

Table (5): Distribution of central vein sign and para-magnetic rim on SWI

Variable	Present (n, %)	Absent (n, %)
Central Vein Sign on SWI	45 (90.0%)	5 (10.0%)
Para-magnetic Rim on SWI	37 (74.0%)	13 (26.0%)

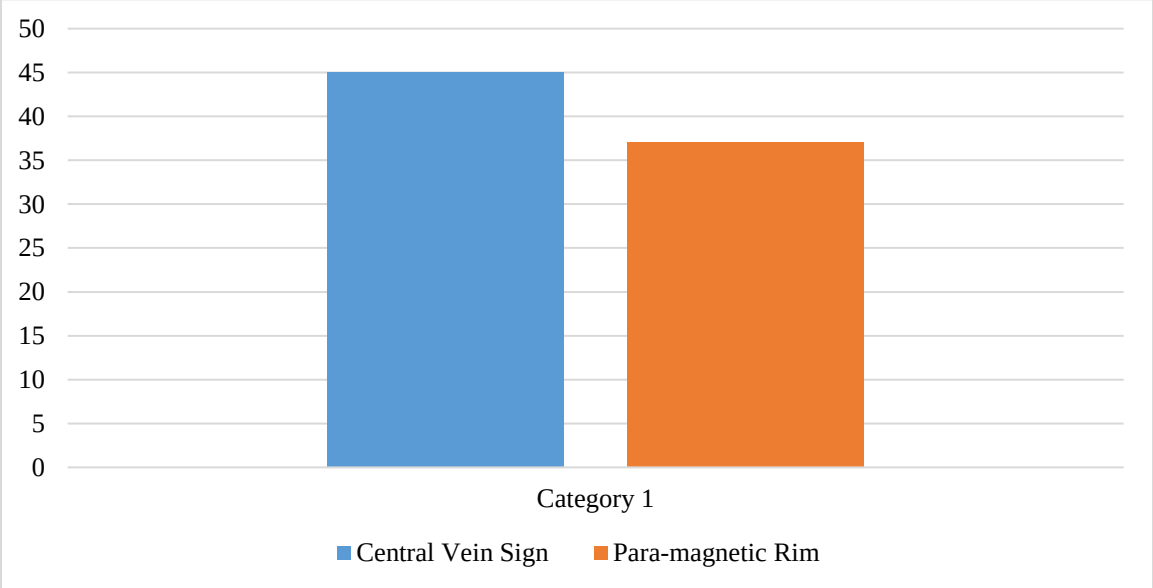

Figure (3): Distribution of central vein sign and para-magnetic rim on SWI

CASES

Case (1): A 29-years-old male with frequent headache received a final MS diagnosis following an initial MRI interpretation suggesting an inflammatory demyelinating process. **Axial 3D FLAIR** images demonstrated multiple bilateral periventricular demyelinating hyperintense foci. Importantly, the **axial SWI** sequence provided enhanced specificity by distinctly visualizing a **paramagnetic rim sign** in one periventricular lesion and a **central vein sign** in another. This outcome exemplified the complementary value of the modalities, where FLAIR establishes the total lesion burden and SWI confirms the presence of characteristic MS-related pathology.

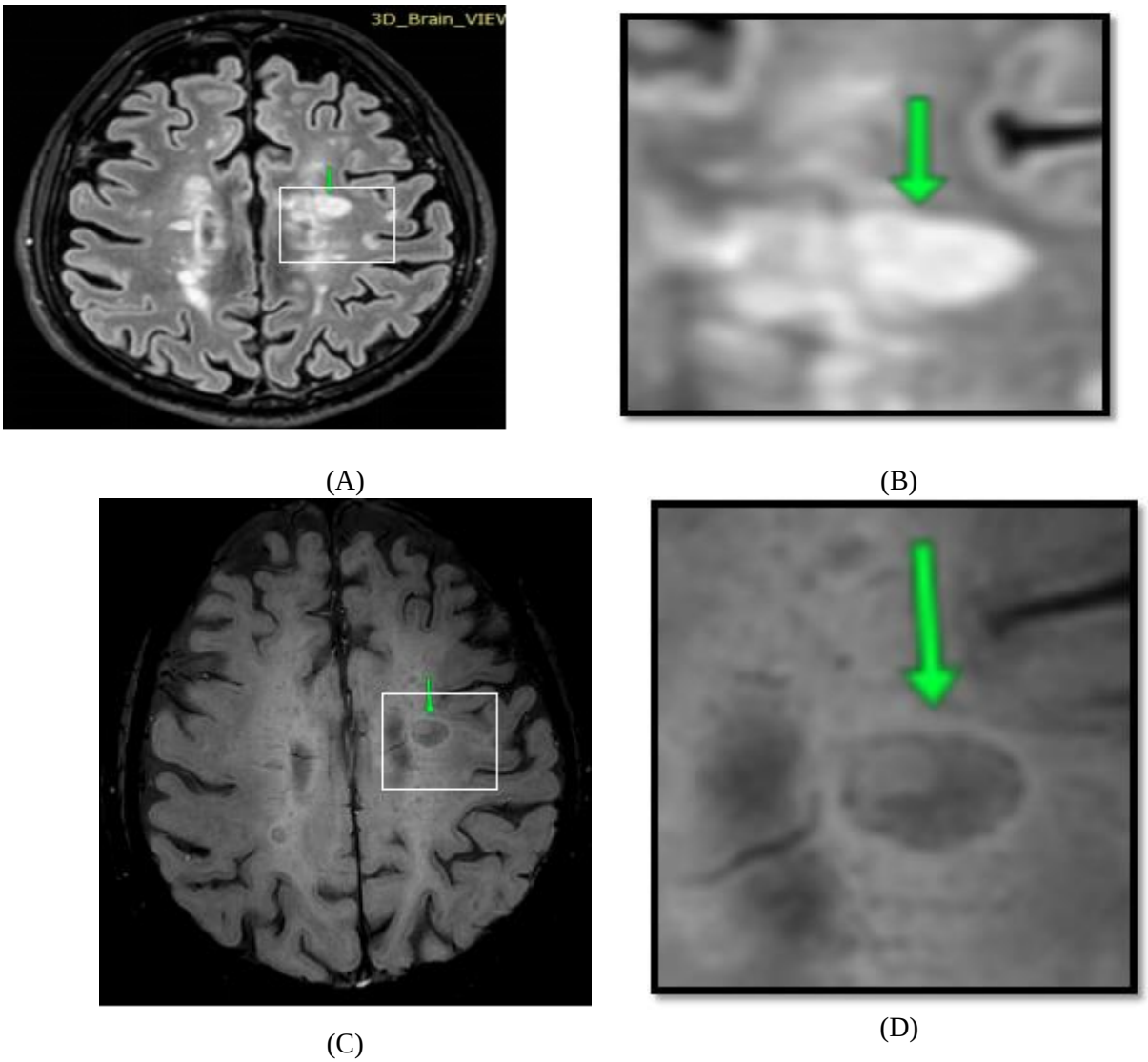

Figure (4): A) Axial 3D FLAIR showed multiple bilateral periventricular demyelinating hyperintense foci. (Arrow). B) A sagittal periventricular demyelinating hyperintense focus. (Arrow). C) Axial SWI paramagnetic rim sign (green arrow) was clearly demonstrated in one of the periventricular lesions. D) Axial SWI central vein sign (black arrow) was clearly demonstrated in one of the periventricular lesions.

CASE (2): A 43-years-old male presenting with nystagmus was ultimately diagnosed with MS. 3D FLAIR revealed a periventricular lesion that exhibited the CVS. Nevertheless, the SWI sequence yielded a significantly more evident CVS within a periventricular lesion, and notably, successfully visualized the central vein in a FLAIR-bright lesion that was undetectable on 3D FLAIR. This finding substantiated the superior sensitivity of SWI for detecting the CVS, which is a pivotal diagnostic biomarker, even when FLAIR successfully identifies the lesion itself.

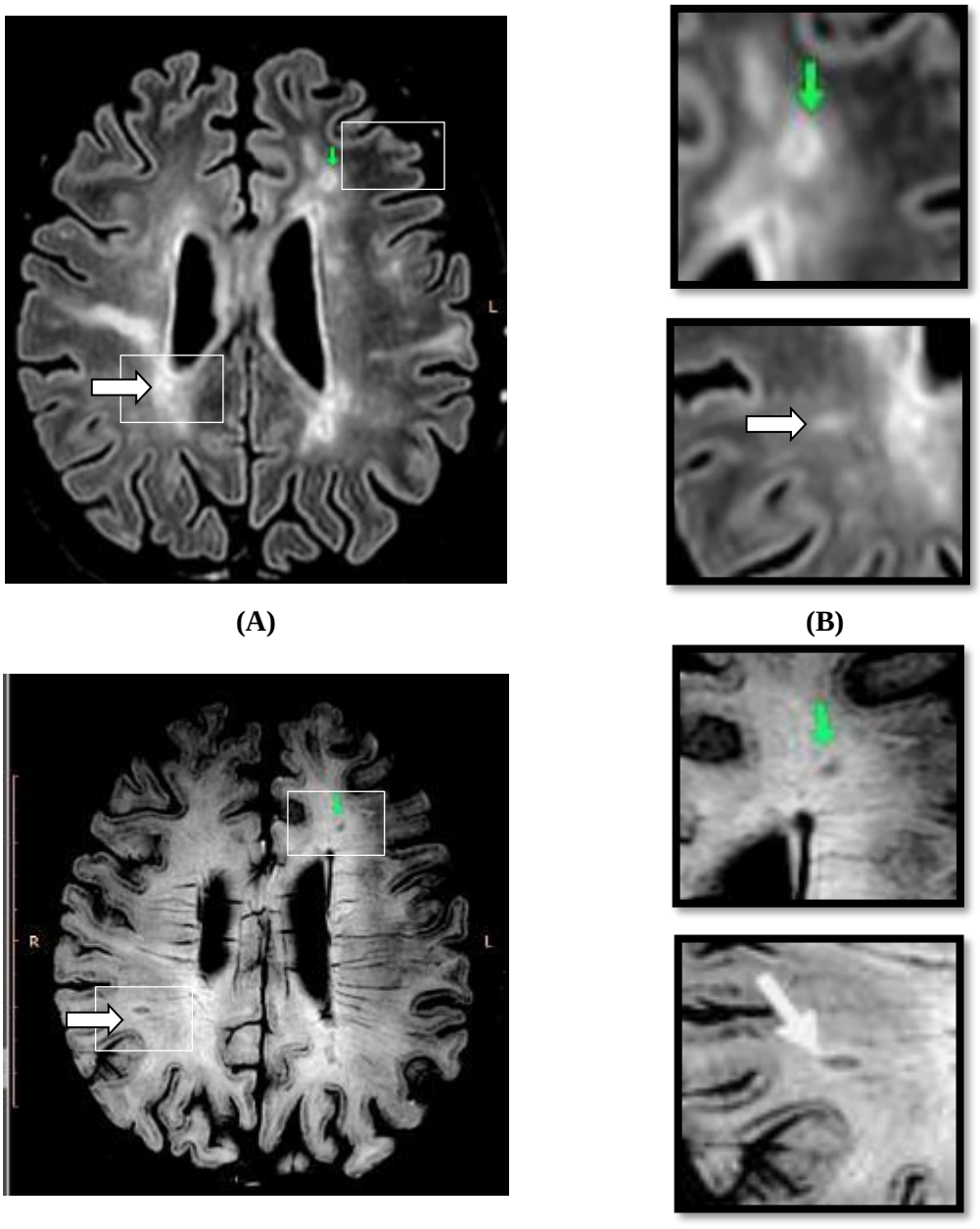

(A) **(B)**

(C) **(D)**

Figure (5): A) An axial periventricular lesion (green arrow) demonstrated the central vein sign on 3D FLAIR. B) Central vein sign in an axial 3D FLAIR periventricular lesion. C) A periventricular lesion demonstrating the central vein sign on SWI, which is much higher than that on 3D FLAIR. D) A FLAIR bright lesion seen on 3D FLAIR, which failed to show the central vein that was clearly visualized on SWI.

CASE (3): A 20-years-old female complaining of vertigo was confirmed to have MS, with the initial MRI reporting an inflammatory demyelinating disease. Axial SWI identified a periventricular lesion displaying a rim of susceptibility. This finding was pathologically corroborated by a rim of enhancement observed on post-contrast T1 imaging, which was also associated with high signal on Diffusion-Weighted Imaging (DWI) and corresponding low signal on the Apparent Diffusion Coefficient (ADC) map, consistent with diffusion restriction. This correlation underscores the importance of the susceptibility rim in identifying lesions with chronic active inflammation, as observed within the study cohort.

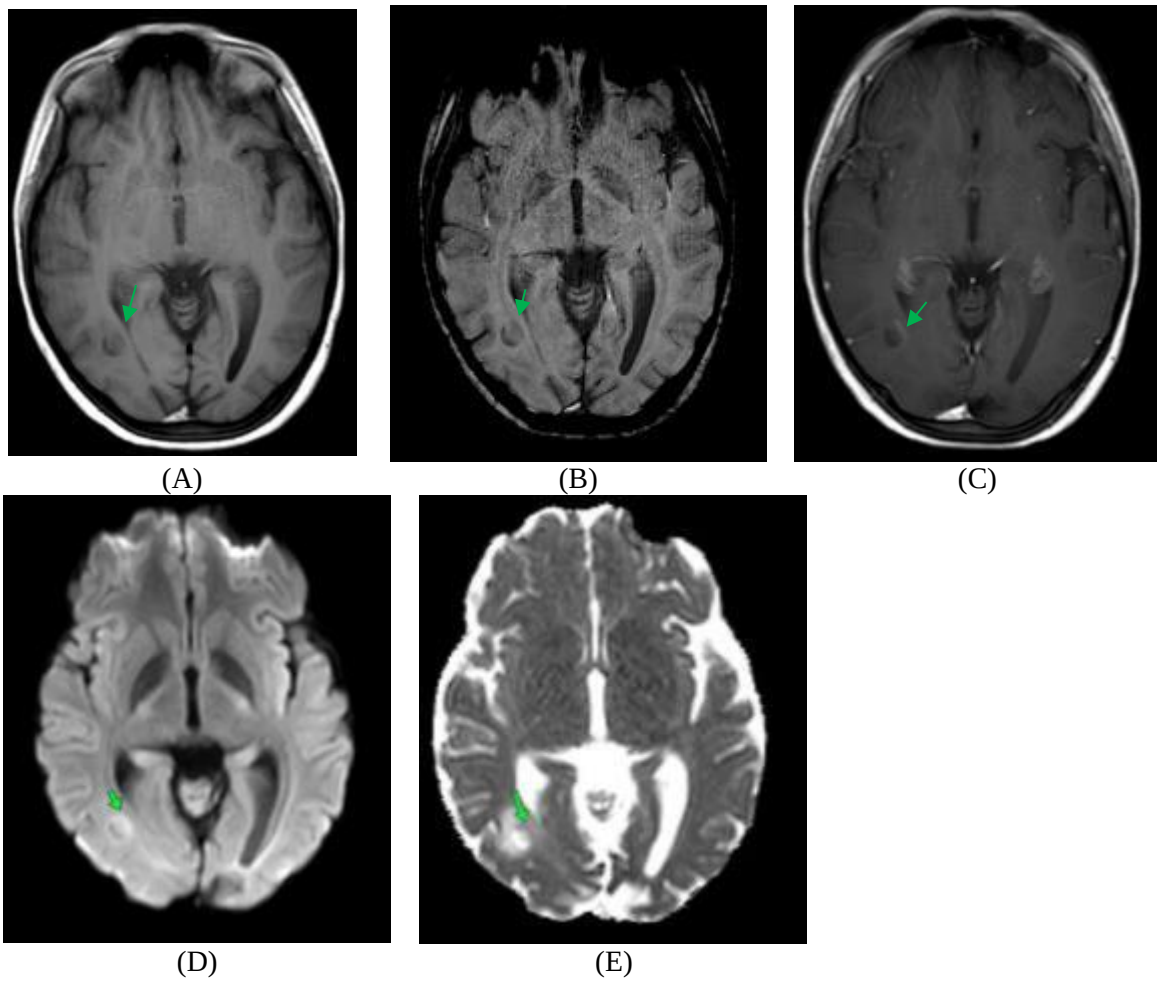

Figure (6): A) periventricular lesion (green arrow) demonstrated a rim of susceptibility on SWI. B) T1 Pre-contrast axial cut of the lesion. C) A rim of enhancement was seen on post contrast T1 of the same lesion. D) This rim also corresponded to high signal on DWI. E) Low signal on ADC map represented diffusion restriction.

Case (4): A 42-year-old female who presented with paraplegia was diagnosed with MS. 3D FLAIR images depicted multiple periventricular lesions, one of which demonstrated the central vein sign. However, another FLAIR-bright lesion did not clearly display the CVS on 3D FLAIR. Subsequently, the SWI sequence provided a more evident central vein sign in one of the lesions compared to 3D FLAIR. This case further supports the conclusion that while 3D FLAIR maintains high sensitivity for overall lesion enumeration, SWI offers augmented specificity in visualizing the CVS, a feature critical for the differentiation of MS from radiological mimics.

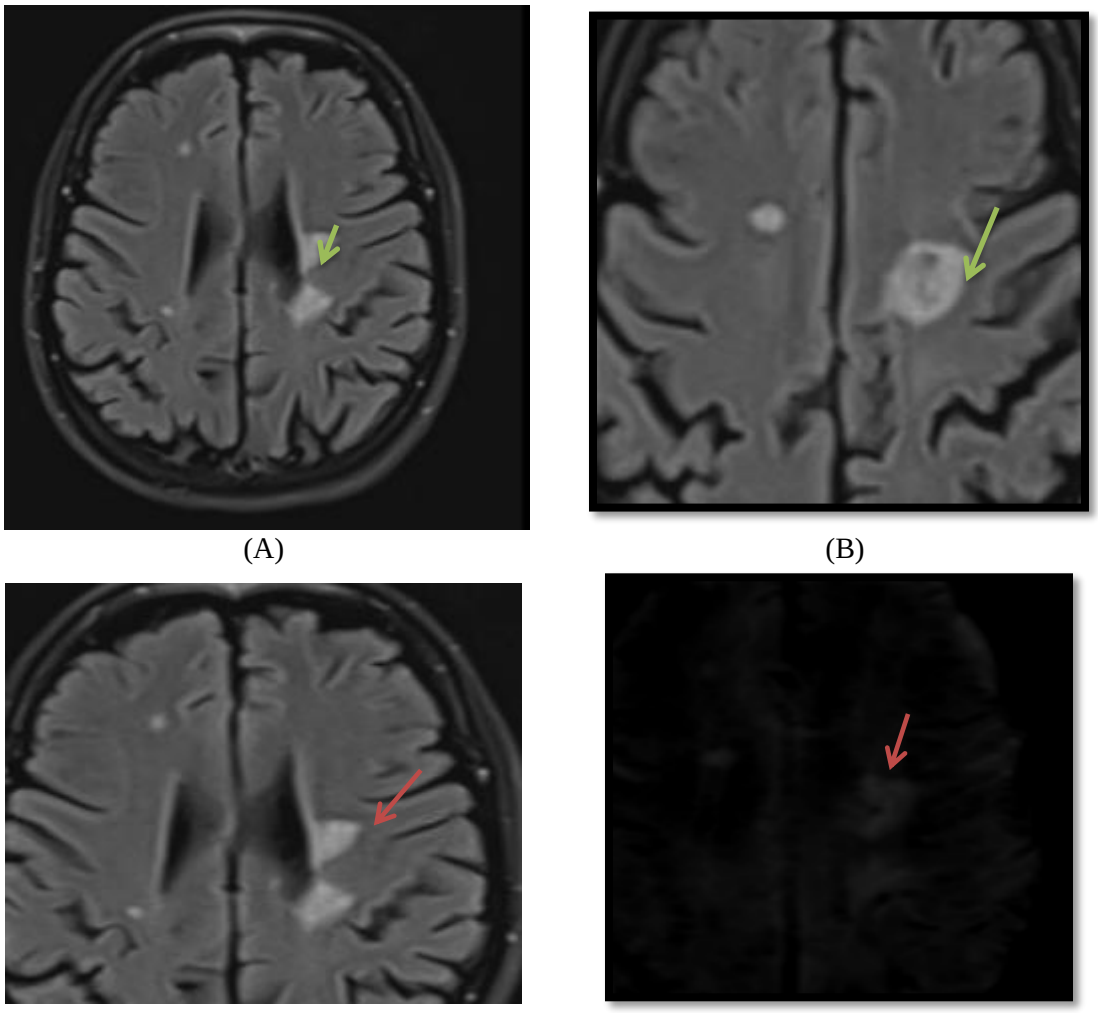

(A) (B)

(C) (D)

Figure (7): A) A periventricular lesion (green arrow) demonstrated the central vein signs on 3D FLAIR. B) Central vein sign closer view on axial 3D FLAIR. C) Another FLAIR bright lesion was seen on 3D FLAIR, which fails to show the central vein sign. D) SWI showing central vein sign in one of the lesions more evident compared to 3D FLAIR.

DISCUSSION

Susceptibility-weighted imaging (SWI) provides complementary information to standard MRI sequences in evaluating Multiple Sclerosis (MS). Although 3D FLAIR and T2-weighted sequences remain the standard for MS lesion detection reflecting edema, demyelination, gliosis and axonal injury, SWI also detects additional aspects of pathology not visible with standard imaging. [15] Highlighted the continued utility of standard MRI in demonstrating lesion dissemination in time and space. Consistent with this, our study demonstrated that 3D FLAIR identified slightly more total lesion numbers and per-patient median lesion numbers than SWI, confirming its increased sensitivity for lesion visibility. However, SWI has unique advantages by capitalizing on tissue magnetic susceptibility differences to image venous anatomy and iron deposition. Iron deposits, either in the form of hemosiderin or ferritin, are reported to accumulate in chronic inflammatory lesions and contribute to oxidative damage and myelin destruction [16].

In our study, SWI was better than FLAIR in depicting vascular and iron-related abnormalities such as the Central Vein Sign (CVS) and paramagnetic rim lesions (PRLs). Specifically, CVS was detected in 90% of patients and PRLs in 74%, underscoring SWI's role in identifying lesion characteristics indicative of chronic inflammation. The detection of CVS is clinically significant as it aids in distinguishing MS from mimics, including small-vessel ischemic disease. SWI's heightened sensitivity to deoxygenated blood enhances venous visualization and facilitates CVS detection [17]. Concomitantly, PRL, that is, iron-laden microglia and macrophages, correlates with overall lesion burden and can be biomarkers for chronic active lesions) [16, 18]. The number of PRLs in this study was highly correlated with total lesion load, and they were useful markers of ongoing compartmentalized inflammation. These results align with earlier researches where **Mohamed *et al.* [19]** and **Zivadinov *et al.* [20]** reported that SWI and quantitative susceptibility mapping (QSM) were capable of detecting vascular disease and iron deposition, which are age-related and related to disease duration.

In our study, SWI identified CVS on multiple occasions in stages of disease, being helpful both in acute and chronic MS. Systematic reviews and meta-analyses also validate the universal inclusion of susceptibility sequences in MS imaging protocols due to their sensitivity and capacity for detection of subtle pathology not identifiable with conventional sequences [21, 22].

Interestingly, SW enhances, but does not replace, contrast-enhanced imaging. Gadolinium-enhanced imaging will detect lesions of active blood–brain barrier disruption, but most PRLs are non-enhancing and reflect chronic, smoldering inflammation [20, 23]. In our subcohort, few PRLs were enhanced with contrast, but SWI accurately detected these consistently, suggesting that SWI could be used as a non-contrast method for detecting chronic inflammatory activity [24]. Higher-generation SWI techniques optimize its diagnostic capability. QSM and sophisticated sequences like IR-SWIET optimize visualization of cortical and subpial lesions and quantitative iron deposition measurement. Each modality provides complementary information: CVS shows vascular involvement, while PRLs show chronic inflammation activity. Together, they maximize diagnostic yield as well as prognostic assessment [18, 25].

From the clinician's perspective, the employment of SWI with routine sequences provides a comprehensive evaluation of MS. While, FLAIR would be ideal for the identification of hyperintense lesions and overall lesion burden, SWI is helpful in providing specificity through highlighting of vascular and iron deposits-related findings. The blend enables the differentiation of mimics, the identification of chronic active lesions and potential monitoring of disease change. Additionally, in patients with contraindications to gadolinium, SWI is a valuable non-contrast salvage for the identification of clinically relevant lesions [25].

Thus, SWI significantly enhances the value of conventional MRI in MS evaluation by showing vascular, iron-contingent and chronic inflammation-contingent lesions not detected on standard sequences. The combination of FLAIR for lesion enumeration and SWI for the identification of vascular and iron-sensitive lesions provides a better characterization of disease burden, change, and lesion pathology, which justifies its routine inclusion in MS imaging protocols.

CONCLUSION

This study shed light on the valuable role of susceptibility-weighted imaging (SWI) in the assessment of Multiple Sclerosis (MS), highlighting its excellence in the visualization of Central Vein Sign (CVS) and paramagnetic rim lesions, two valuable imaging markers with diagnostic and prognostic value. While, 3D FLAIR remains more sensitive to the detection of overall lesion burden, SWI is more specific particularly in the detection of features associated with active inflammation and chronic disease activity. The fact that CVS was present in 90% of the patients and paramagnetic rims in 74% highlighted the potential of SWI as an adjunct to standard MRI sequences. The capacity of SWI to unveil iron pathology gives insight into MS lesion pathodynamics and can potentially differentiate MS from other white matter disorders.

Funding: None.
Conflict of interest: None.

REFERENCES

1. **Papiri G, D'Andreamatteo G, Cacchiò G *et al.* (2023):** Multiple Sclerosis: Inflammatory and Neuroglial Aspects. Curr Issues Mol Biol., 45 (2): 1443-1470.
2. **Elsalam S, Salah S, Said A *et al.*(2024) :**Differentiating multiple sclerosis from cerebral small vessel disease using diffusion tensor imaging and magnetic resonance spectroscopy on normally appearing thalami. *Egyptian Journal of Radiology and Nuclear Medicine*, *55*(1):12.
3. **Eisele P, Szabo K, Griebe M *et al.* (2012):** Reduced diffusion in a subset of acute MS lesions: a serial multi-parametric MRI study. AJNR Am J Neuroradiol., 33: 1369-1373.
4. **Tomassini V, Sinclair A, Sawlani V *et al.* (2020):** Diagnosis and management of multiple sclerosis: MRI in clinical practice. J Neurol., 267 (10): 2917-2925.
5. **Clarke M, Pareto D, Pessini-Ferreira L *et al.* (2020):** Value of 3T Susceptibility-Weighted Imaging in the Diagnosis of Multiple Sclerosis. AJNR Am J Neuroradiol, 41 (6): 1001-1008.
6. **Sahraian M, Eshaghi A (2010):** Role of MRI in diagnosis and treatment of multiple sclerosis. Clin Neurol Neurosurg, 112 (7): 609-615.
7. **Anan R, El-Adalany M, Belal T, Elmogy S (2020) :** Detection of central veins using susceptibility weighted imaging (SWI) for discrimination between lesions in multiple sclerosis (MS) and cerebral small vessel disease (CSVD). *Egyptian Journal of Radiology and Nuclear Medicine*, *51*(1): 63.
8. **Rubin A, Waszczuk Ł, Trybek G *et al.* (2022):** Application of susceptibility weighted imaging (SWI) in diagnostic imaging of brain pathologies – a practical approach. Clin Neurol Neurosurg., 221: 107368.
9. **Castellaro M, Tamanti A, Pisani A(2020):** The use of the central vein sign in the diagnosis of multiple sclerosis: a systematic review and meta-analysis. *Diagnostics*, *10*(12): 1025.
10. **Sinnecker T, Clarke M, Meier D *et al.* (2019):** Evaluation of the Central Vein Sign as a Diagnostic Imaging Biomarker in Multiple Sclerosis. JAMA Neurol., 76 (12): 1446.
11. **Halefoglu A, Yousem D (2018):** Susceptibility weighted imaging: Clinical applications and future directions. World J Radiol., 10 (4): 30-45.
12. **Brownlee W, Vidal-Jordana A, Shatila M(2025):** Towards a unified set of diagnostic criteria for multiple sclerosis. *Annals of neurology*, *97*(3): 571-582.
13. **Simon J, Li D, Traboulsee A *et al.* (2006):** Standardized MR imaging protocol for multiple sclerosis: Consortium of MS Centers consensus guidelines. AJNR Am J Neuroradiol., 27 (2): 455-461.
14. **Clarke M, Cheek R, Kazimuddin H *et al.* (2024):** Paramagnetic rim lesions and the central vein sign: Characterizing multiple sclerosis imaging markers. J Neuroimaging, 34 (1): 86-94.
15. **Haacke E, Makki M, Ge Y *et al.* (2009):** Characterizing iron deposition in multiple sclerosis lesions using susceptibility weighted imaging. J Magn Reson Imaging, 29 (3): 537-544.
16. **Cai J, Zhang X, Qiao H *et al.* (2015):** Susceptibility-weighted imaging of the venous networks around the brain stem. Neuroradiology, 57 (2): 163-169.
17. **Liu C, Li W, Tong K *et al.* (2015):** Susceptibility-weighted imaging and quantitative susceptibility mapping in the brain. J Magn Reson Imaging, 42 (1): 23-41.
18. **Mohamed A, Rania A, Sabry A *et al.* (2022):** Added value of susceptibility weighted imaging (SWI) in diagnosis of multiple sclerosis (MS). Med J Cairo Univ., 89: 1459-1462.
19. **Zivadinov R, Ramasamy D, Benedict R *et al.* (2016):** Cerebral microbleeds in multiple sclerosis evaluated on susceptibility-weighted images and quantitative susceptibility maps: a case-control study. Radiology, 281 (3): 884-895.
20. **Afkandeh R, Abedi I, Zamanian M (2024):** Detection of multiple sclerosis lesions by susceptibility-weighted imaging—A systematic review and meta-analyses. Clin Radiol., 79 (12): e1522-e1529.
21. **Haller S, Haacke E, Thurnher M *et al.* (2021):** Susceptibility-weighted imaging: technical essentials and clinical neurologic applications. Radiology, 299 (1): 3-26.
22. **Eisele P, Fischer K, Szabo K *et al.* (2019):** Characterization of contrast-enhancing and non-contrast-enhancing multiple sclerosis lesions using susceptibility-weighted imaging. Front Neurol., 10: 1082.
23. **Darwish E, El-Sayed F, Teiba M (2024):** The role of susceptibility weighted imaging as a substitute to post-contrast T1-weighted images in detection of active multiple sclerosis lesions. QJM., 117 (2): 175-918.
24. **Beck E, Gai N, Filippini S *et al.* (2020):** Inversion recovery susceptibility weighted imaging with enhanced T2 weighting at 3 T improves visualization of subpial cortical multiple sclerosis lesions. Invest Radiol, 55 (11): 727-735.
25. **Grabner G, Dal-Bianco A, Schernthaner M *et al.* (2011):** Analysis of multiple sclerosis lesions using a fusion of 3.0 T FLAIR and 7.0 T SWI phase: FLAIR SWI. J Magn Reson Imaging, 33 (3): 543-549.